proceedings

MDPI

Proceedings

Geometrical Parametrization of Piezoelectric Sensors for Acoustical Monitoring in Hadrontherapy †

Jorge Otero [1,*] and Ivan Felis [2]

[1] Institute d'Investigació per a la Gestió Integrada de les Zones Costaneres (IGIC), Universitat Poltècnica de Vàlencia (UPV), 46730 Gandía, València, Spain

[2] Centro Tecnológico Naval y del Mar (CTN), 30320 Fuente Álamo, Murcia, Spain; ivanfelis@ctnaval.com

* Correspondence: jorotve@upv.es; Tel.: +34-986-19-75-21

† Presented at the 6th International Electronic Conference on Sensors and Applications, 15–30 November 2019; Available online: https://ecsa-6.sciforum.net/.

Published: 14 November 2019

Abstract: Hadrontherapy has been constantly evolving in leaps and bounds since the 1950s, when the use of heavy particles was proposed as an alternative treatment to radiotherapy with gamma rays or electrons. The main objective of this treatment is to maximize the dose applied to the tumour, avoiding damage to the surrounding tissue. One of the keys to the success of hadrontherapy is to achieve instantaneous monitoring of the energy deposition in the environment. Since energy deposition leads to the generation of a thermoacoustic pulse, acoustic technologies have been tested with successful results. However, for this purpose, it is essential to increase the sensitivity of the sensors for the acoustical signal and, therefore, to optimize their geometry as a function of the beam that would be used. We have studied a PTZ material in volumetric and surface volumes through experimental measures and FEM methods. In this text, we start with numerical studies which determine the dependence of the thermoacoustic signal frequency with the energy and duration of the hadron beam.

Keywords: hadrontherapy; Bragg peak; piezoelectric devices; optimization of ceramics

1. Introduction

Piezoelectric sensors have been extensively used due to their basic direct and inverse piezoelectric effects, which take part in the relation between electric field and mechanical deformation. A useful piezoelectric geometry is the circular cylindrical shape. It is used in several applications in actuators, sensors for mechanical structures, underwater monitoring, and medical research. Nowadays, one of the main aspects of medical applications is the use of piezoelectric materials in the detection of pressure pulses, produced by a thermoacoustic effect due to the interaction of proton beams in human tissues. In fact, one of the fields of medicine is the use of directed beams of ionizing radiation (electrons, X-ray, protons), whereby radiosurgery is an important method of treatment of malignant tumours and isolated metastases. However, in the case of radiation over healthy tissue, it is a challenge to detect acoustic signals or the energy deposition in small tumours; there are also areas where the radiation is not safe because an over-irradiation in near areas would cause problems for the patients. Hadrontherapy monitoring consists of the detection of the pressure pulse produced as a result of the behaviour of the Bragg peak created by a pulsed proton beam. In those cases, proton-acoustic signals depend on a variety of parameters such as beam pulse width, energy, spot size, and measurement noise. Some studies about the detection limits on proton-acoustic signals in clinical proton therapy scenarios have aimed to determine the detection threshold of the proton-acoustic method. The results set the

limit on the sensitivity of the proton-acoustic method and should establish a quick reference for assessing whether a given irradiation scenario produces a detectable proton-acoustic signal [1].

In previous studies about piezoelectric geometric optimization, the relation between diameter and thickness according to geometry for a unique dimension has been researched [2,3]. Using this information, in this work, an optimization of cylindrical piezoelectric PZT material was developed to improve the sensibility according to the characteristics of the beam and signal-to-noise ratio for a matrix of 36 different diameters and thicknesses. The aim was to modify this geometrical shape to determine the better diameter-thickness ratio for each case and, according to the required frequency, to set up the shape that maximize the sensor sensitivity, mainly in low frequencies. For this, several circular PIC255 piezoelectric ceramics with different widths and heights were studied with analytical and numerical methods and contrasted with experimental measurements. There are previous works with circular PZT where the authors studied the optimization of shape for two fixed shapes, modifying the diameter and thickness [2,3]. With these, the optimization is based on obtaining the better electromechanical coupling factor related with first, second, and third resonance modes. This factor depends on the resonance (f_r) and antiresonance (f_a) frequencies of the electrical impedance and its amplitude. The product of each frequency resonance and the length (thickness (t) or diameter (d)) is associated with the mode of vibration ($f_r \cdot d$ and $f_a \cdot t$) and the piezoelectric coupling factor $k^2 = f_a^2 - f_r^2/f_a^2$ can be obtained. Therewith, the ratio of coupling factor k_1/k_2 in low frequency gives a quantified estimation of the energy distribution. Based on these studies, the method proposed in this paper is to evaluate, with many thicknesses and diameters, the improvement of receiver sensitivity according to the hadrontherapy technique.

2. Numerical Analysis

The optimization of the piezoelectric volume is based on a free bounded circular ceramic. Figure 2 shows the geometrical scheme of a piezoelectric ceramic. The ceramic is polarized through the z axis and the xy surfaces conform the electrodes. The vibration characteristics are obtained from the constitutive equations for piezoelectric materials [4,5]. Of the three different modes of vibration of piezoelectric disks (radial, extensional, tangential and transverse), a theoretical and experimental analysis [6] have demonstrated that only radial vibration mode can be measured in an impedance analysis. For that reason, just an analysis of vibrational characteristics of extensional mode had been carried out. According to some studies [3], the analytical model has been contrasted with simulation data. In these studies, the results have been validated in radial vibration on piezoelectric disks with different diameter–thickness ratios. The impedance curves used to study the behaviour of piezoelectric material were implemented in the COMSOL Multiphysics in Acoustic-Piezoelectric Interaction module. In this software, the size of tetrahedral meshing elements—i.e., its smaller wavelength—was taken into account, and it was discretized in almost ten parts. A mechanical free boundary condition was set in all the contours of the transducer and uniformly electrical open-circuit voltages were set to the electrodes. The voltage applied on the electrodes was set up in 500 mV and the polarized direction corresponded with the thickness of the shape (z axis). The geometry of the shapes simulated depended on the frequency produced by the set-up parameters in the hadrontherapy applications. In these cases, frequencies between 50 and 350 kHz were studied. For this reason, diameters and thicknesses from 5 to 40 mm every 1 mm were proposed. In total, 1296 simulations were completed to get results in optimization.

Optimization Method

In previous studies, the optimization of the volume in a piezoelectric ceramic has been applied to 1 diameter and 1 thickness [2]. In that case, the numerical results for radial and thickness vibration were taken from the relationship between diameter and thickness. However, in this paper, only the radial mode has been borne in mind because the frequencies studied in hadrontherapy applications are reproduced in low frequency mode. A scheme of optimization method is shown in Figure 1, where the input and the output of the required functions are described. This optimization method was split into four stages, which sum up the relation between the piezoelectric device parameters and the

hadrontherapy parameters, and how it has been related according to the frequency. As for the first step form the piezoelectric device, a radius and thickness contribute to the radial vibrational mode, whereby a relationship between the geometry of the ceramic and the frequency could be written as [7] $N_p = f_r/d$ and $N_t = f_r/th$, where N_p and N_t represent the frequency constant which for PZT PIC255 material is 2000. The N_p expression gives the analytical resonance frequency in radial and thickness vibrational modes. According to different studies, these frequencies vary between 60 kHz and 380 kHz in accord with input parameters typical in hadrontherapy simulations. Using the expression for N_p and N_t, the diameter and thickness ranges were set up between 4 and 40 mm. These lengths covered the bandwidth and were also the input parameters in the model. Once the input parameters had been defined, in Step 2 the impedance modulus was exported from the numerical model for each frequency, in which the minimum value in impedance represented the resonance frequency and the maximum value of the impedance represented the antiresonance frequency in the first and second radial modes, respectively. As will be seen later, for each pair of resonance and antiresonance frequencies in the first and second mode, the electromechanical coupling coefficient could be obtained.

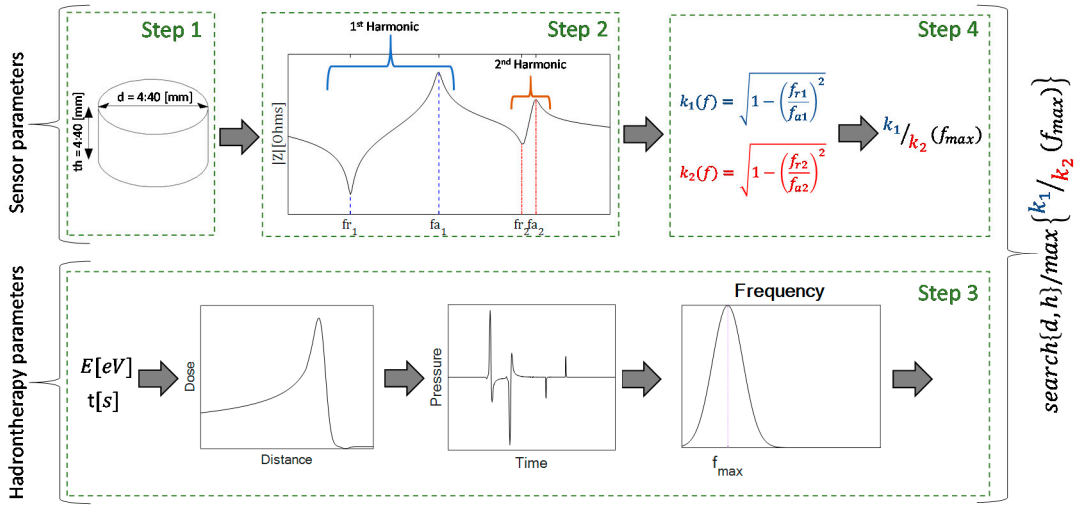

Figure 1. Input parameters for different diameters and thicknesses that produce output parameters.

The thermoacoustic parameters can be evaluated carefully in different experimental and analytical studies [1,8–11]. To sum up, the energy of the beam and the temporal profile are the input parameters in the Bragg peak [12] and thermoacoustic model [11]. As a result, in Step 3, the proton interacts with the tissue and the resulting Bragg peak behaviour produces a pressure in the PTZ sensor, whose amplitude is related to the number of protons per pulse [1] and the frequency of the temporal profile of the source.

Due to the frequency results in the thermoacoustic model, it was possible to relate the hadrontherapy parameters with the piezoelectric device characteristics. In Step 4, the electromechanical coupling coefficient was calculated for the first two modes and a relation of those is shown as k_1/k_2. On the one hand, once a respective frequency has been obtained from the thermoacoustic model, the region where resonance and antiresonance frequencies fit with the maximum in the electromechanical coupling coefficient will be the best match to the diameter-thickness ratio. Considering that there are some values in the region of the k_1/k_2 that could fit the solution, in this paper k_1/k_2 has been evaluated as the maximum frequency in the thermoacoustic model.

3. Experimental Setup

To compare the numerical solution, a measurement of electrical impedance was made. For this case, the method described in [2] was used in piezoelectric disks. The bandwidth frequency impedance response was measured of PIC255 piezoceramics with diameter $D = 10$ mm and thickness $t =$

5 mm. The measurements were done through the resonance method using a Wayner Kerr Electronics 6500PLF impedance analyser. The electrodes were located in each surface on the ceramic in air. Figure 2 shows the ceramic and the experimental setup.

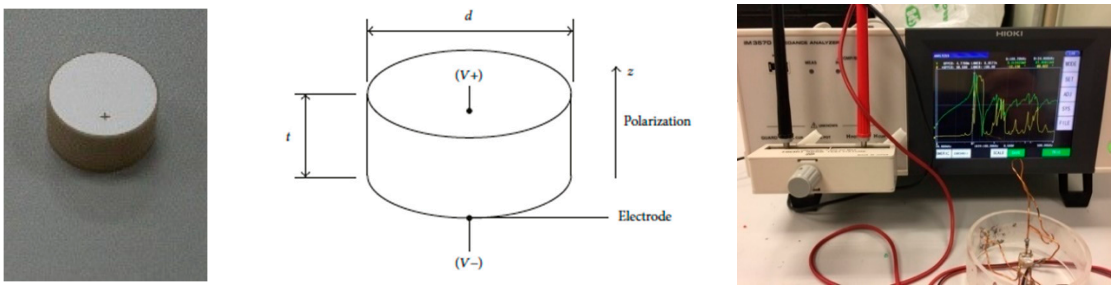

(**a**) (**b**)

Figure 2. (**a**) Piezoelectric disc with 10 mm diameter and 5 mm thickness with longitudinal polarization; (**b**) experimental set up to measure the electrical impedance in piezoelectric elements.

When the ceramic is excited in a resonance frequency of radial vibration, the value of the impedance reaches a minimum. As a result, the modulus of the impedance provides information about the resonance and antiresonance frequencies for each vibration mode.

4. Results

4.1. Resonance and Antiresonance Behaviour

According to the theorical electrical impedance modulus, Figure 3 shows the typical behaviour of a piezoelectric ceramic disc in radial mode vibration. The local minimum and maxima appearing in the impedance curve correspond to resonance and antiresonance frequency respectively. Figure 3a shows numerical and measured results in the transducers studied ($d = 10$ mm and $t = 5$ mm). The frequency starts in numerical simulation and experimental measurement were 100 Hz to 500 kHz, with an increase step of 100 Hz as measured by a Wayne Kerr impedance analayzer. Figure 3b also shows the relationship between the resonance f_r and antiresonance f_a frequencies, diameter, and thickness of the transducer for the first mode for the numerical simulation.

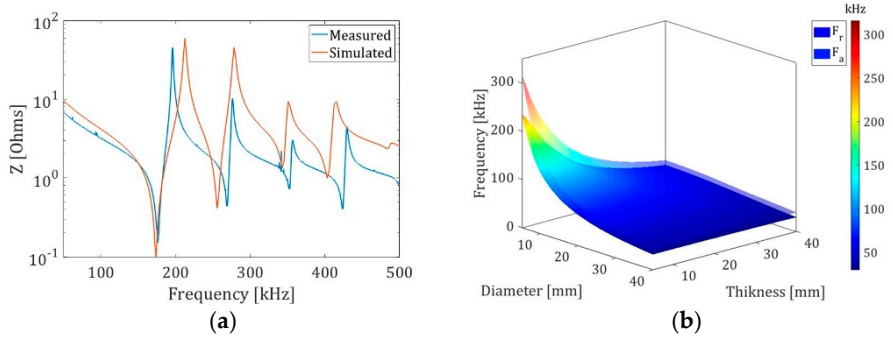

(**a**) (**b**)

Figure 3. (**a**) Comparison in impedance modulus form FEM simulations and measurement; (**b**) resonance and antiresonance results of simulations to different diameters and thicknesses.

In low frequency, the analytical and numerical fits gave positive results in the bandwidth studied for applications in hadrontherapy [1]. The resonance frequency increased with decreasing diameter in a nonlinear relationship, as shown in Figure 3.

4.2. Electromechanical Coupling Coefficient

The electromechanical coupling coefficient is a measure of the effectiveness with which electrical energy is converted into mechanical energy and vice versa. It was proposed by Manson and is obtained by measuring the resonance and antiresonance frequencies through the expression $k =$

$\sqrt{1-(f_r/f_a)^2}$. This coefficient is a reference to the design of piezoelectric ceramics and it is expressed in values between 0 to 1. Figure 4 shows the value for the electromechanical coupling coefficient for the first and second low frequency modes in function of diameter and thickness.

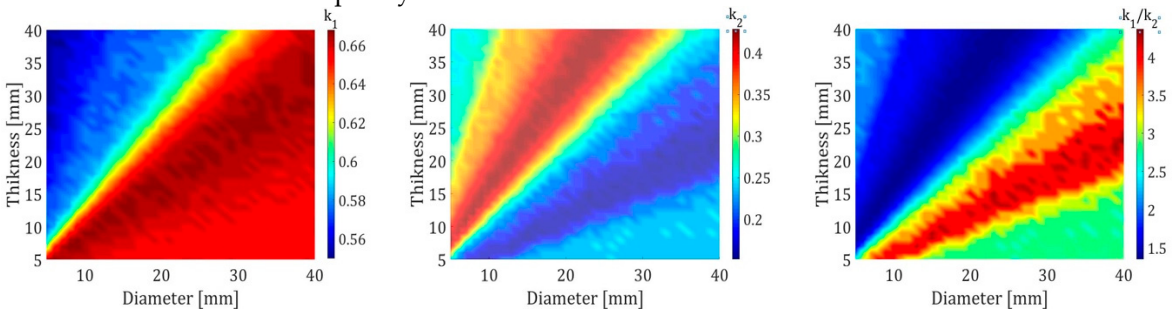

Figure 4. Ratio between the electromechanical coupling coefficient k of the first and second lower modes as a function of diameter and edge thickness. (**a**) Electromechanical coupling coefficient in the firs lower mode $(k_{1st.mode})$ in 2D; (**b**) electromechanical coupling coefficient in the second lower mode $(k_{2nd.mode})$ in 2D view; (**c**) k_1/k_2 ratio electromechanical coupling coefficient in 2D.

In general, the best efficiency energy fit for the lowest radial mode takes place when the diameter is larger than the thickness. With this graphic, is possible to predict the behaviour of the frequency of a disk ceramic in response to an improving resonance frequency. Figure 4c shows the ratio of the electromechanical coupling factor of the first mode $(k_{1st.mode})$ to that of the second mode $(k_{2nd.mode})$. A high variation in the ratios between the electromechanical coupling coefficient k happened due to the different nature of the modes observing values of k_1/k_2 up to 4.0. Lower resonance frequencies corresponding with the radial mode and a relatively low coefficient k_1/k_2 (about 1.2), thanks to a great interaction between modes, resulted in a more homogeneous response in this frequency. According to the simulations, there are some geometries that meet the frequency requirements of a small volume, low frequency and reduced k_1/k_2, depending on the applications.

5. Discussion and Conclusions

In order to have a first approximation of this optimization problem, this study was developed to develop a tool for optimizing piezoelectric sensor design for hadrotherapy applications. The study compared the behaviour of a piezoelectric ceramic that was measured in a laboratory and simulated according to a previously planned method. This study is a continuation of research into radial extensional modes in piezoelectric disks with mechanical free boundaries evaluated with numerical simulations and experimental measurements [2]. To validate the effects of this paper, we have analysed some research on the theoretical detection of the proton acoustic signal [1,8–10] to improve the Received Voltage Response (RVR). The low-pressure amplitudes in hadrontherapy applications present a challenge in the use of ultrasound sensors to adapt protoacoustic measurements for protoacoustic verification. These low-pressure amplitudes are caused by tissue heterogeneity in acoustic reflection, absorption, refraction, and changes in the medium velocity, all of which distort the pressure wave shape and increase the error in signal detection. For a beam energy of 100 MeV, a pulse width of 5 µs, a spot size of 10 mm, and $5.0 \cdot 10^6$ protons per pulse, the central frequency is 128 kHz [1]. Therefore, in this case, the pressure in the sensor at 20 mm from the Bragg peak is 0.2 Pa. If we take a plane where it cut the resonance frequency and antiresonance frequency, is possible to choose the best geometric fit. Figure 5a shows an evaluated plane with a frequency of 128 kHz.

Once the intersection points (where the plane matches a resonance frequency and antiresonance frequency) are defined, it is possible to determine the values of diameter and thickness which are the best fit with this frequency. In the electromechanical coupling coefficient ratio, it is possible to find the maximum value at which these sizes match with the best frequency fit. As a result of the analysis, the RVR is obtained for each specific case. Table 1 in Figure 6 shows the values of diameter and thickness in these intersection points for the resonance and antiresonance frequencies. According to the electromechanical coupling coefficient ratio, the best fit to optimize the sensibility in 128 kHz is in a

disk with a diameter ($D = 15$ mm) and a thickness ($t = 9$ mm) where the relationship between k_1/k_2 is at its maximum. Figure 6 shows a new geometry to improve the sensitivity. The experimental (red line) and simulated (black line) RVR for a ceramic studied is shown where the RVR corresponding with -185 dB in frequency was studied. In addition, the new geometrical fix matched with a diameter ($D = 15\,mm$) and thickness ($t = 9$ mm) presented a substantial improvement at the same frequency with a value of -171 dB.

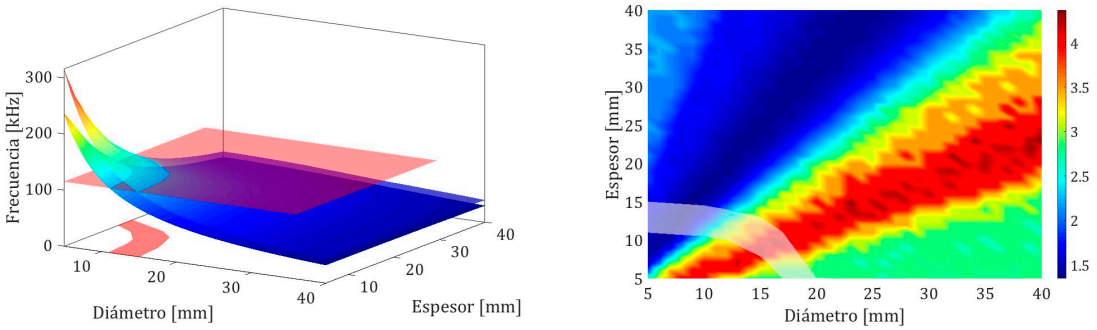

Figure 5. Optimization method. (**a**) Resonance and antiresonance results show the area where the planes are cut, in this case at 128 kHz; (**b**) k_1/k_2 electromechanical coupling coefficient ratio which is being cut by the frequency's area.

Table 1. Diameter and thickness intersection points for resonance and antiresonance frequencies.

Resonance Frequency	Diameter [mm]	5–13
	Thickness [mm]	5–20
Anti-Resonance Frequency	Diameter [mm]	5–17
	Thickness [mm]	5–24

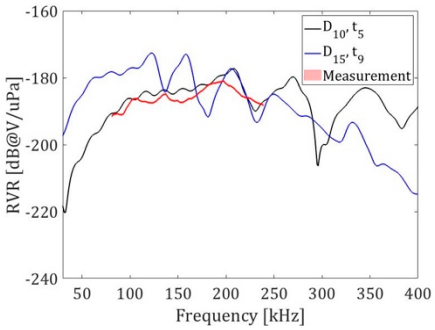

Figure 6. Left: range of geometries where a 110 kHz frequency could improve the sensibility in PZT material; right: received voltage response (RVR) for simulations ceramics.

Taking into account that elecomechanical coupling k indicates a different interation between first and second modes for different radius and thickness values, the studies and results presented here are especially relevant for low frequencies near first and second resonance modes. Minor changes in the size of the material produced maximums and minimums in the RVR that were more significant when the resonance frequencies in shapes' diameter and thickness coincided with each other. In consequence, when first and second resonance modes are closer, there is a maximum in the relation k_1/k_2 for the frequency evaluated, which entails an increase in the sensibility in that frequency. In this region, the maximum values that form the k_1/k_2 ratio were near 4.5. These results show a significant contrast between the efficiency of the first two modes of the ceramic. On the plus side, Figure 5 shows that there was also a noticeable increase in the sensitivity in the bandwidth below 200 kHz. The way forward to find the best fit is to have a better relationship in the bandwidth in low frequency, based on the maximum frequency of hadrontherapy applications. This would create the possibility of increased sensibility below that maximum frequency. To sum up, it is possible to establish a method to improve the received voltage response (RVR) according to the frequency requirements in hadrontherapy applications. It would be useful to optimize the volume in piezoelectric sensors considering the compromise between low k_1/k_2.

Conflicts of Interest: The authors declare no conflict of interest.

References

1. Ahmad, M.; Xiang, L.; Yousefi, S.; Xing, L. Theoretical detection threshold of the proton-acoustic range verification technique. *Med. Phys.* **2015**, *42*, 5735–5744.
2. Ardid, M.; Felis, I.; Martínez-Mora, J.A.; Otero, J. Optimization of Dimensions of Cylindrical Piezoceramics as Radio-Clean Low Frequency Acoustic Sensors. *J. Sens.* **2017**, *2017*, 8179672.
3. Felis. Tecnologías Acústicas para la Detección de Materia Oscura. Diseño y desarrollo de un detector Geyser. Ph.D. Thesis, Universidad Politécnica de Valencia, Valencia, Spain, 2017.
4. Kunkel, H.A.; Locke, S.; Pikeroen, B. Finite-Element Analysis of Vibrational Modes in Piezoelectric Ceramic Disks. *IEEE Trans. Ultrason. Ferroelectr. Frequency Control* **1990**, *37*, 316–328.
5. Sun, D.; Wang, S.; Hata, S.; Shimokohbe, A. Axial vibration characteristics of cylindrical, radially polarized piezoelectric transducer with different electrode patterns. *Ultrasonics* **2010**, *50*, 403–410.
6. Huang, C.H.; Lin, Y.C.; Mia, C.C. Theoretical Analysis and Experimental Measurement for Resonance Vibration of Piezoceramic Circular Plates. *IEEE Trans. Ultrason. Ferroelectr. Frequency Control* **2004**, *51*, 12–24.
7. APC. *Piezoelectric Ceramics: Principles and Applications*; APC International: Mackeyville, PA, USA, 2011.
8. Jones, K.C.; Witztum, A.; Sehgal, C.M.; Avery, S. Proton beam characterization by proton-induced acoustic emission: Simulation studies. *Phys. Med. Biol.* **2014**, *59*, 6549–6563.
9. Graf, K.; Anton, G.; Hössl, J.; Kappes, A.; Karg, T.; Katz, U.; Lahmann, R.; Naumann, C.; Salomon, K.; Stegmann, C. Testing thermo-acoustics sound generation in water with proton and laser beams. *Int. J. Mod. Phys. A* **2006**, *21*, 127–131.
10. Jones, K.C.; Seghal, C.M.; Avery, S. How proton pulse characteristics influence protoacoustic determination of proton-beam range: Silumation studies. *Phys. Med. Biol.* **2016**, *61*, 2213–2242.
11. Assmann, W.; et al. Ionoacoustic characterization of the proton Bragg peak with submillimeter accuracy. *Med. Phys.* **2015**, *42*, 567–574.
12. Bragg, W.H.; Bragg, W.L. The reflection of X-rays by Crystals. *Proc. R. Soc. A* **1913**. doi:10.1098/rspa.1913.0040
13. Kanazawa, K.; Yoon, S.M.; Chao, N. Analyzing spur distorted impedance spectra for the QCM. *J. Sens.* **2009**, *2009*, 259746.